

UCLA

UCLA Previously Published Works

Title

Differential effects of PD-1 and CTLA-4 blockade on the melanoma-reactive CD8 T cell response

Permalink

<https://escholarship.org/uc/item/8dk368s5>

Journal

Proceedings of the National Academy of Sciences of the United States of America, 118(43)

ISSN

0027-8424

Authors

Gangaev, Anastasia
Rozeman, Elisa A
Rohaam, Maartje W
et al.

Publication Date

2021-10-26

DOI

10.1073/pnas.2102849118

Peer reviewed



Differential effects of PD-1 and CTLA-4 blockade on the melanoma-reactive CD8 T cell response

Anastasia Gangaev^a, Elisa A. Rozeman^{a,b,1}, Maartje W. Rohaan^{a,b,1}, Olga I. Isaeva^{a,c,d,1}, Daisy Philips^a, Sanne Patiwaal^a, Joost H. van den Berg^a, Antoni Ribas^e, Dirk Schadendorf^f, Bastian Schilling^{f,g}, Ton N. Schumacher^{a,d}, Christian U. Blank^{a,b}, John B. A. G. Haanen^{a,b}, and Pia Kvistborg^{a,2}

^aDivision of Molecular Oncology & Immunology, The Netherlands Cancer Institute, Amsterdam, 1066 CX, The Netherlands; ^bDepartment of Medical Oncology, The Netherlands Cancer Institute, Amsterdam, 1066 CX, The Netherlands; ^cDepartment of Tumor Biology & Immunology, The Netherlands Cancer Institute, Amsterdam, 1066 CX, The Netherlands; ^dOncode Institute, Utrecht, 3521 AL, The Netherlands; ^eUniversity of California Los Angeles Jonsson Comprehensive Cancer Center, University of California, Los Angeles, CA 90095; ^fDepartment of Dermatology, University Hospital Duisburg-Essen, Essen D-45147, Germany; and ^gDepartment of Dermatology, Venereology, and Allergology, University Hospital Würzburg, Würzburg 97080, Germany

Edited by James P. Allison, The University of Texas MD Anderson Cancer Center, Houston, TX, and approved September 3, 2021 (received for review February 16, 2021)

Immune checkpoint inhibitors targeting programmed cell death protein 1 (PD-1) and cytotoxic T lymphocyte-associated protein 4 (CTLA-4) have revolutionized the treatment of melanoma patients. Based on early studies addressing the mechanism of action, it was assumed that PD-1 blockade mostly influences T cell responses at the tumor site. However, recent work has demonstrated that PD-1 blockade can influence the T cell compartment in peripheral blood. If the activation of circulating, tumor-reactive T cells would form an important mechanism of action of PD-1 blockade, it may be predicted that such blockade would alter either the frequency and/or the breadth of the tumor-reactive CD8 T cell response. To address this question, we analyzed CD8 T cell responses toward 71 melanoma-associated epitopes in peripheral blood of 24 melanoma patients. We show that both the frequency and the breadth of the circulating melanoma-reactive CD8 T cell response was unaltered upon PD-1 blockade. In contrast, a broadening of the circulating melanoma-reactive CD8 T cell response was observed upon CTLA-4 blockade, in concordance with our prior data. Based on these results, we conclude that PD-1 and CTLA-4 blockade have distinct mechanisms of action. In addition, the data provide an argument in favor of the hypothesis that anti-PD-1 therapy may primarily act at the tumor site.

PD-1 | CTLA-4 | melanoma-reactive CD8 T cells

Immune checkpoint–targeting therapies, in particular those targeting the programmed cell death protein 1/ligand 1 (PD-1/PD-L1) axis, now form the standard of care for advanced melanoma (1) and a number of other solid cancers including non–small cell lung cancer (NSCLC) (2), renal cell carcinoma (3), and urothelial carcinoma (4). Despite the widespread clinical use of PD-1/PD-L1 blocking agents, the mechanism by which these therapies enhance immune-mediated tumor control remains incompletely understood. Early work addressing the mechanism of action of PD-1 blockade showed increased numbers of intratumoral proliferating (Ki-67⁺) CD8 T cells and T cell receptor (TCR) clones after treatment (5). These findings provide evidence for a boosting effect on tumor-infiltrating CD8 T cells. In line with these findings, PD-L1 expression on tumor cells has been shown to have predictive value for therapy outcome (5–7) and influence the activity of PD-1 blockade in at least some mouse models (8, 9). Other studies, however, have suggested that PD-1 blockade may also exert its effect through activation of circulating tumor-reactive CD8 T cell responses. First, studies in mouse models of chronic viral infection have shown the recruitment of CXCR5⁺ Tim-3⁻ CD8 T cells from the white pulp of the spleen upon PD-1 blockade (10, 11). Second, data obtained using mouse tumor models demonstrated that the proliferative response to anti-PD-1 therapy is dependent on CD28-mediated costimulation (12), and these findings

are in line with a mechanistic study showing that PD-1 signaling inhibits T cell functionality through attenuation of CD28 costimulation (13). Collectively, the latter findings have been interpreted as PD-1 blockade potentially having a role in inducing proliferation of the tumor-reactive CD8 T cell pool. Recent data from clinical studies in patients provide evidence supporting such a hypothesis. First, NSCLC and melanoma patients treated with PD-1 blockade showed an increase in proliferating (Ki-67⁺) CD8 T cell subsets (14–17). Second, PD-1 blockade was shown to result in clonal replacement of tumor-infiltrating CD8 T cells in patients with squamous cell carcinoma (18). In contrast, however, an analysis of peripheral blood from melanoma patients showed no consistent increase in TCR diversity after treatment (19). Although the current knowledge suggests that PD-1 blockade may alter the circulating tumor-reactive CD8 T cell compartment, direct evidence for such a hypothesis is currently lacking.

Importantly, most studies that have addressed the impact of PD-1 blockade on CD8 T cells focused the analyses on bulk CD8 T cells without assessing the T cell specificity. However,

Significance

Despite the success of checkpoint-targeting therapies, many melanoma patients do not respond or acquire resistance after initial responsiveness. A better understanding about the mechanism by which these therapies enhance immune-mediated tumor control is key to providing the rationale for better treatment strategies. In this study, we show that PD-1 blockade does not modulate the breadth or the magnitude of the circulating tumor-reactive CD8 T cell response. In contrast and in concordance with our previous study, CTLA-4 blockade leads to a broadening of the circulating melanoma-reactive CD8 T cell response. Together, these findings show differential mechanisms of action of CTLA-4 and PD-1 blockade and support the synergy of the combination treatment seen in the clinic.

Author contributions: A.G., T.N.S., J.B.A.G.H., and P.K. designed research; A.G., E.A.R., M.W.R., D.P., S.P., and P.K. performed research; T.N.S. contributed new reagents/analytic tools; A.G., E.A.R., M.W.R., O.I.I., D.P., J.H.v.d.B., A.R., D.S., B.S., C.U.B., and P.K. analyzed data; A.G. and P.K. wrote the paper; E.A.R., M.W.R., J.H.v.d.B., and A.R. provided patient material and clinical data; and D.S., B.S., C.U.B., and J.B.A.G.H. provided clinical samples and clinical data.

The authors declare no competing interest.

This article is a PNAS Direct Submission.

Published under the PNAS license.

¹E.A.R., M.W.R., and O.I.I. contributed equally to this work.

²To whom correspondence may be addressed. Email: p.kvistborg@nki.nl.

This article contains supporting information online at <http://www.pnas.org/lookup/suppl/doi:10.1073/pnas.2102849118/-DCSupplemental>.

Published October 20, 2021.

work from Schreiber and colleagues has shown that “bystander” CD8 T cells respond differentially to checkpoint-targeting therapies compared to tumor-reactive CD8 T cells in their mouse model (20). These findings demonstrate the importance of dissecting the mechanism of action of checkpoint-targeting therapies on the tumor-reactive CD8 T cell response rather than the bulk CD8 T cell compartment. In this study, we assessed whether PD-1 blockade can increase the magnitude of preexisting melanoma-reactive CD8 T cells (boosting) and/or lead to newly detectable tumor-reactive CD8 T cell responses (broadening) in peripheral blood of melanoma patients (Fig. 1A).

Results

Kinetics of the Melanoma-Reactive CD8 T Cell Response during PD-1 Blockade. To determine which on-therapy time point would allow us to evaluate therapy-induced alterations, we first assessed the kinetics of melanoma-reactive CD8 T cell responses before and during PD-1 blockade. For this purpose, peripheral blood samples from six melanoma patients were collected pretherapy and at three on-therapy time points between week 3 and week 17 of treatment. The melanoma-reactive CD8 T cell response was analyzed using a panel of peptide major histocompatibility complex (pMHC) multimers loaded with 71 different epitopes derived from previously described shared melanoma antigens and restricted to human leukocyte antigen (HLA)-A*02:01 (Fig. 1B and *SI Appendix, Fig. S1A and Table S1*). CD8 T cells reactive toward these epitopes were identified by the combinatorial encoding of pMHC multimers using a unique dual fluorochrome code for each of the 71 epitopes, and all responses were confirmed using a different color-code combination in each of the two independent experiments (*SI Appendix, Fig. S1 B and C*). We identified a total of seven melanoma-reactive CD8 T cell responses in five of six patients (Fig. 1 C and D). An increase in magnitude (defined as \geq twofold) was found in four of the seven identified CD8 T cell responses. In one of the five patients in which melanoma-reactive CD8 T cell responses were detected, three newly detectable (gained) melanoma-reactive CD8 T cell responses were identified. Two of these gained responses were detected at all analyzed on-therapy time points. Together, these data suggested that potential effects of anti-PD-1 therapy in terms of the broadening and/or boosting of the circulating melanoma-reactive CD8 T cell response can be detected at the time of the first clinical response evaluation around week 12.

PD-1 Blockade Does Not Alter the Circulating, Melanoma-Reactive CD8 T Cell Response. To systematically assess potential alterations in terms of the boosting and/or broadening of the melanoma-reactive CD8 T cell response upon anti-PD-1 therapy, we included pre- and on-therapy (time of first clinical evaluation; median: week 12 and range: week 6 to 17) samples from 18 additional patients, resulting in a sample set of 24 patients. For all 48 samples, T cell reactivities toward the 71 melanoma-associated epitopes were analyzed, resulting in more than 3,400 individual analyses of antigen-specific CD8 T cell responses. Melanoma-reactive CD8 T cell responses were found in 19 of the 24 patients. The median magnitude of these responses ($n = 27$) was 0.019% (range: 0.005 to 0.920%) of total CD8 T cells (Fig. 2 A and B). CD8 T cell reactivity was found toward seven of the 71 melanoma-associated epitopes (9%) including epitopes derived from overexpressed antigens (PRDX5 and Meloe-1), cancer/germline antigens (MAGE-A3), and melanocyte-differentiation antigens (gp100, MART-1, and Tyrosinase). Furthermore, in line with prior studies in HLA-A*02:01⁺ melanoma patients (21, 22), CD8 T cells reactive toward MART-1 were found in the vast majority of patients (79%). Strikingly, the magnitude of preexisting melanoma-

reactive CD8 T cell responses was unaltered upon therapy with a median fold change of 1.2 ($P = 0.26$), demonstrating the lack of a substantial boosting effect (Fig. 2C). Furthermore, newly detected responses (gained) were only observed in three of the 24 patients ($P = 0.25$, Fig. 2D). These data show that the frequency and the breadth of the circulating melanoma-reactive CD8 T cell response was not substantially altered upon PD-1 blockade. As a technical control for the generation of pMHC multimers, two viral epitopes derived from the Epstein-Barr virus and influenza A were included in the analysis. A total of 24 virus-specific CD8 T cell responses were detected in 20 of the 24 patients, and no significant alterations in the magnitude of these responses upon anti-PD-1 therapy were observed (*SI Appendix, Fig. S2 A and B*; $P = 0.86$).

PD-1 Blockade Does Not Alter the TCR Repertoire of Circulating CD8 T Cells. Based on the pMHC multimer data, we did not observe alterations of the circulating melanoma-reactive CD8 T cell response upon anti-PD-1 therapy in most patients. This assay is limited to a panel of shared melanoma antigens restricted to the HLA-A*02:01 allele. To further investigate CD8 T cell repertoire-wide changes upon PD-1 blockade, we assessed the TCR repertoire dynamics of circulating bulk CD8 T cells isolated from peripheral blood samples collected before and during anti-PD-1 therapy (same time point as used for pMHC multimer assay) from five patients in which at least one melanoma-reactive CD8 T cell response was identified using the pMHC multimer technology. Sequencing of the TCR β -chain complementarity-determining region 3 (CDR3) revealed a high level of similarity of the TCR repertoires (Morisita-Horn overlap index: median: 0.94 and range: 0.91 to 0.97) between pre- and on-therapy samples in all five patients (Fig. 3A). Only a low percentage (median: 0.14% and range: 0.06 to 0.34%) of shared TCR clonotypes were found to be differentially expressed between pre- and on-therapy samples in all patients (Fig. 3B). These findings were further supported by similar distributions of the V-segment gene usage and the CDR3 length between pre- and on-therapy samples (Fig. 3 C and D). Finally, no significant differences in TCR repertoire clonality were found (Fig. 3E; $P = 0.19$). Next, we examined previously identified TCR β -chain CDR3 sequences specific for antigens restricted to HLA-A*02:01 that were included in the pMHC multimer screen (*SI Appendix, Table S1*) and those matching all previously identified sequences linked to specificity for shared tumor and viral antigens regardless of the HLA restriction element. In line with the pMHC multimer data, TCR sequences specific for MART-1 (ELAGIGILTV), EBV (GLCTLVAML), and influenza A (GILGFVFTL) were not significantly altered upon PD-1 therapy (*SI Appendix, Fig. S3 A and B*). Similarly, all TCR β -chain CDR3 sequences with established antigen specificity identified in our data showed no significant alterations in the number of reads or the number of clones upon anti-PD-1 therapy (*SI Appendix, Fig. S3 C and D*). In line with the pMHC multimer data, these data demonstrate that PD-1 blockade does not induce significant repertoire-wide changes of the circulating CD8 T cell response.

PD-1 Blockade Does Not Alter the Circulating Melanoma-Reactive and CXCR5⁺ Tim-3⁻ CD8 T Cell Compartment. Previous studies have shown that anti-PD-1 therapy can induce proliferation of CXCR5⁺ Tim-3⁻ CD8 T cells which are recruited from the white pulp of the spleen in mice with chronic viral infection (10, 11), and similar subsets responsive to anti-PD-1 therapy have been identified in tumor models (23, 24). A change in the frequency of this subset has only been detected early after the start of anti-PD-1 therapy (day 7 to 10 on-therapy) (16). Similarly, data from melanoma patients showed a transient increase in proliferation of PD-1⁺ CD8 T cell subsets in peripheral blood at week 1

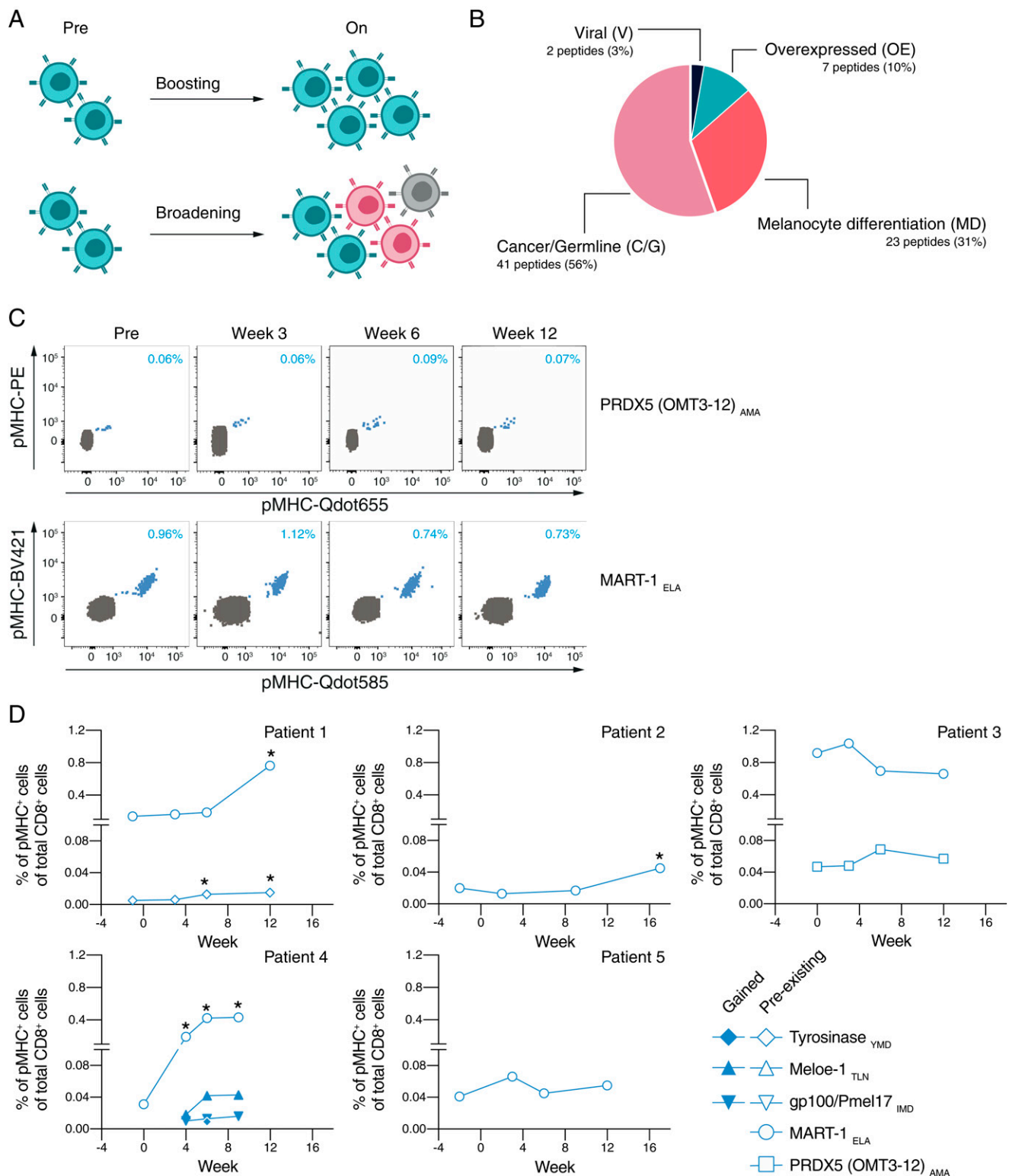


Fig. 1. Hypothesis and kinetics of melanoma-reactive CD8 T cell responses during anti-PD-1 therapy. (A) Potential mechanisms of anti-PD-1 therapy include expansion of preexisting tumor-reactive CD8 T cells (boosting) and induction of novel, tumor-reactive CD8 T cell responses (broadening). (B) Overview of the HLA-A*02:01-restricted epitope panel. A total of 71 shared melanoma-associated epitopes were included to analyze the tumor-reactive CD8 T cell responses. Viral epitopes served as positive control for the generation of pMHC multimers. Detailed information about the epitopes is provided in *SI Appendix, Table S1*. (C) Representative flow cytometry plots of melanoma-reactive CD8 T cell responses (blue, located in the diagonal of the plot because of the dual coding strategy) before and during anti-PD-1 therapy. The magnitude of melanoma-reactive CD8 T cell responses (blue, upper right corner) represents the percentage of total CD8 T cells (gray). A representative example of the full gating strategy is provided in *SI Appendix, Fig. S1*. (D) Kinetics of melanoma-reactive CD8 T cell responses detected in melanoma patients ($n = 5$) following anti-PD-1 therapy. A \geq twofold increase (on-therapy versus pretherapy) in magnitude is indicated (*).

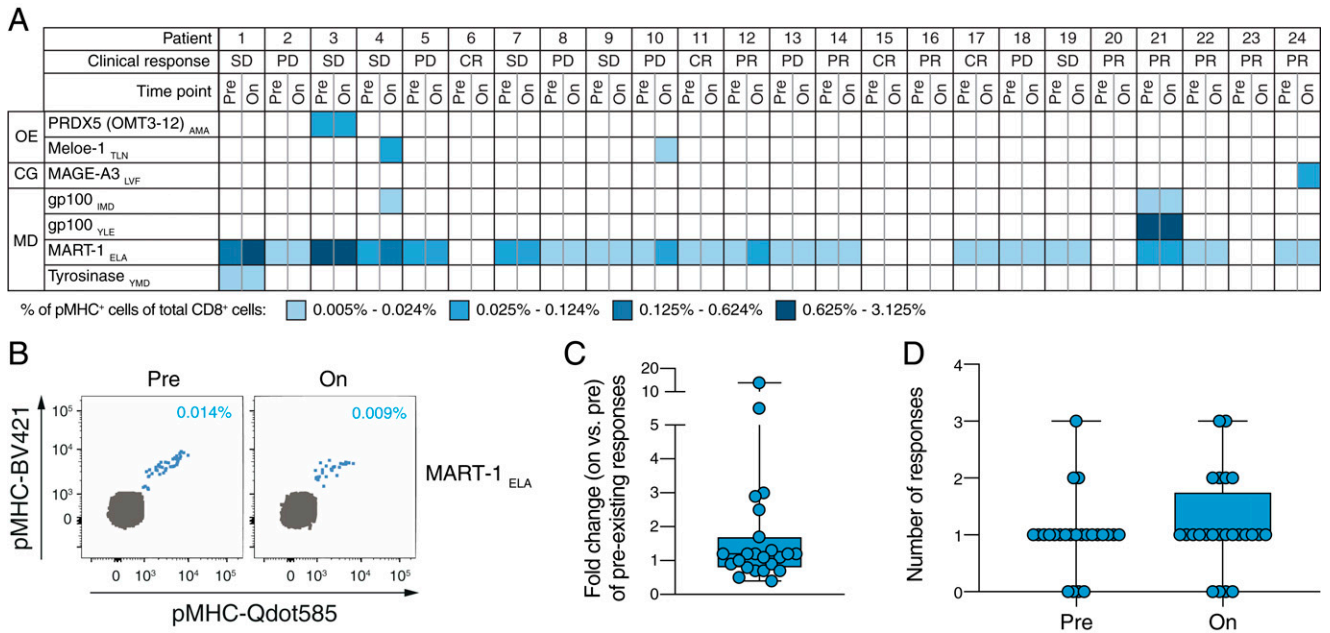


Fig. 2. Large-scale analysis of the melanoma-reactive CD8 T cell response upon PD-1 therapy. (A) Heatmap overview of melanoma-reactive CD8 T cell responses ($n = 27$) detected in melanoma patients ($n = 24$) before and during (median: week 12, range: week 6 to 17) anti-PD-1 therapy. OE: overexpressed, C/G: cancer/germline, MD: melanocyte differentiation, SD: stable disease, PD: progressive disease, PR: partial response, CR: complete response. (B) Representative flow cytometry plots of a melanoma-reactive CD8 T cell response (blue) detected in peripheral blood pre- and on-anti-PD-1 therapy. Magnitude of the melanoma-reactive CD8 T cell response (blue, upper right corner) is indicated on the top right as the percentage of total CD8 T cells (gray). A representative example of the full gating strategy is provided in *SI Appendix, Fig. S1*. (C) Fold change in the magnitude of preexisting melanoma-reactive CD8 T cell responses ($n = 23$) after anti-PD-1 therapy. Boxplot represents the median and interquartile ranges, and the whiskers represent the full range. Statistical significance for a change in magnitude on-therapy, as compared to pretherapy, was tested with a two-tailed Wilcoxon signed-rank test, $P = 0.26$. (D) Number of responses detected in each individual patient ($n = 24$) pre- and on-anti-PD-1 therapy. Boxplots represent the median and interquartile ranges, and the whiskers represent the full range. Statistical significance for a change in the number of responses on-therapy as compared to pretherapy was tested with a two-tailed Wilcoxon signed-rank test, $P = 0.25$.

after treatment initiation (16). Together, these findings suggest that PD-1 blockade may induce a systemic effect based on the priming and recruitment of CD8 T cells from lymphoid organs. To test this hypothesis, we collected peripheral blood samples from eight melanoma patients at week 1 in addition to pretherapy and week 12 samples. First, we examined alterations in the frequency of the CXCR5⁺ Tim-3⁻ CD8 T cell subset that was previously identified in mice (10, 11). In contrast to chronic viral infection and mouse tumor models, we observed no significant changes in the frequency of CXCR5⁺ Tim-3⁻ CD8 T cells in peripheral blood of melanoma patients at either week 1 or at week 12 after the start of therapy (Fig. 4 A and B and *SI Appendix, Fig. S4*). Second, we assessed changes of the melanoma-reactive CD8 T cell response in 4 HLA-A*02:01⁺ patients. A total of six melanoma-reactive CD8 T cell responses were found in three of these four patients (Fig. 4C and *SI Appendix, Fig. S5*). For two of the three patients, no significant alterations in the magnitude of preexisting CD8 T cell responses were found at either week 1 or at week 12. Significant alterations in the magnitude were only detected in one patient (patient 21) in which all three responses showed a transient increase at week 1. Similarly, only one newly induced response was found in one patient (patient 25) at week 1; however, this response was of very low magnitude (0.008% of total CD8) and just above the cutoff (0.005% of total CD8 T cells) of the technology. Overall, we observed no consistent boosting or broadening of the circulating, melanoma-reactive CD8 T cell response at week 1.

The Characteristics of the Analyzed Patient Cohort Are Comparable to Previous Studies. To understand whether our patient cohort was representative to previously analyzed cohorts, we first

examined the clinical outcome of the patients analyzed in this study. Previously, reported response rates to anti-PD-1 therapy in stage IV melanoma patients range from 35 to 40% across multiple studies (25). The objective response rate in the current study cohort was 50% (Table 1). In the vast majority of patients with clinical benefit (10/12), no changes in magnitude or breadth of the circulating, melanoma-reactive CD8 T cell response were observed (*SI Appendix, Table S2*). Alterations of the melanoma-reactive CD8 T cell response were observed in a minority of patients (including two responders and two nonresponders), and a direct comparison between responders and nonresponders showed no significant differences in terms of boosting ($P = 0.99$) or broadening ($P = 0.99$) of the melanoma-reactive CD8 T cell response (*SI Appendix, Fig. S6 A and B*). Of note, 14 of the 24 patients included in this study received anti-CTLA-4 therapy prior to anti-PD-1 therapy (Table 1). In line with previous studies (5, 26), the clinical response rate to anti-PD-1 therapy was lower in anti-CTLA-4 pretreated patients (21%) compared to patients without prior anti-CTLA-4 therapy (90%). However, no significant differences in terms of boosting ($P = 0.13$) or broadening ($P = 0.99$) of the melanoma-reactive CD8 T cell response upon anti-PD-1 therapy were found between patients with and without prior anti-CTLA-4 therapy (*SI Appendix, Fig. S6 C and D*). The time since the last dose of anti-CTLA-4 therapy (median: 6 and range: 1 to 24 mo) was not correlated ($P = 0.21$) with the fold change in magnitude of preexisting melanoma-reactive CD8 T cell responses upon anti-PD-1 therapy (*SI Appendix, Fig. S6E*). Noteworthy, although nonsignificant ($P = 0.12$), preexisting responses in samples collected before anti-PD-1 therapy were found in most patients (93%) with prior anti-CTLA-4

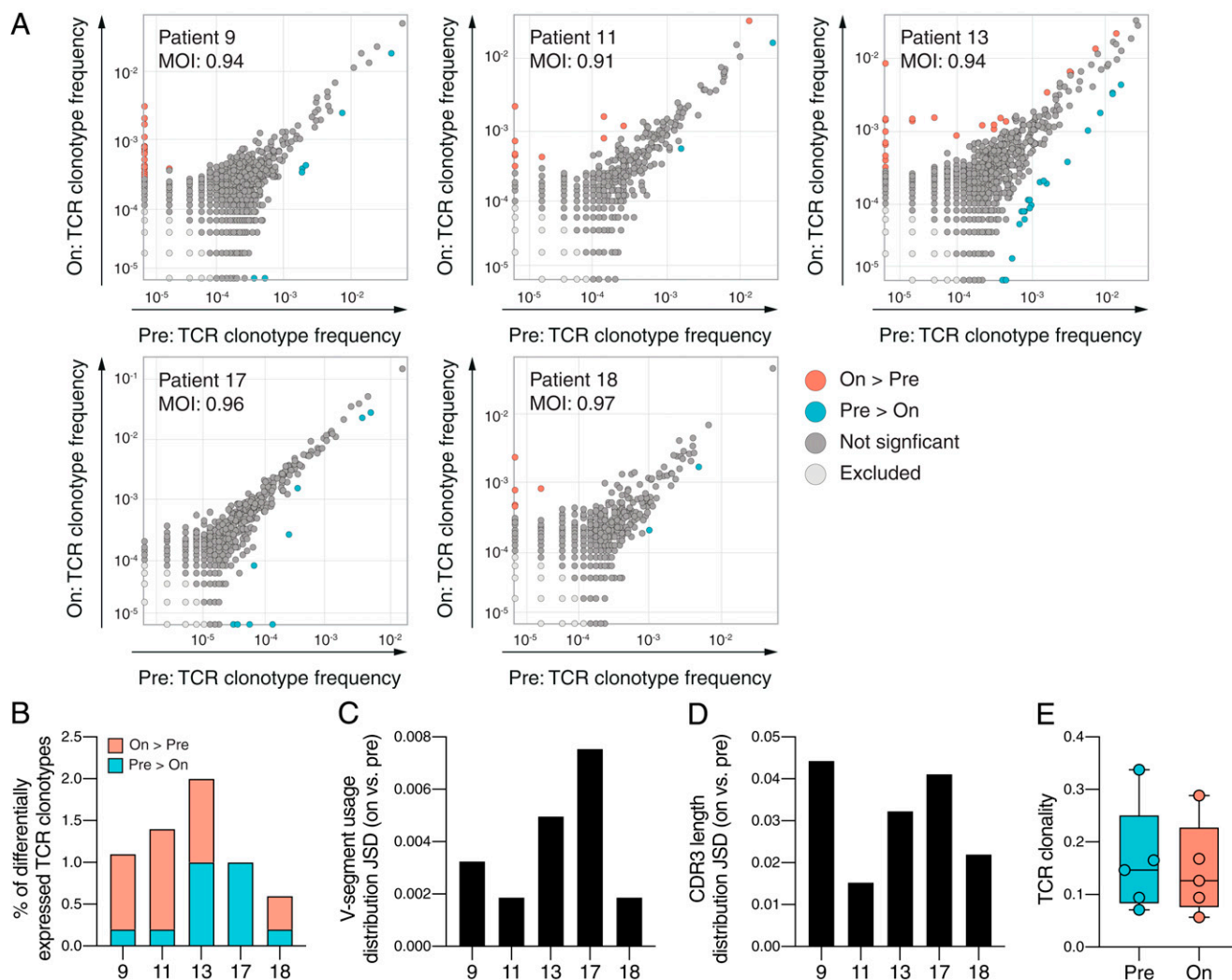


Fig. 3. Analysis of the TCR repertoire of circulating CD8 T cells upon anti-PD1 therapy. (A) Distribution of the CD8 TCR β -chain CDR3 clonotype abundance in pre- and on-therapy samples for each individual patient ($n = 5$). Dots represent the TCR β -chain CDR3 clonotypes detected within a single repertoire in pre- and on-therapy samples. TCR β -chain CDR3 clonotypes that are significantly overrepresented in on- and pretherapy are indicated in red and blue, respectively. The Morisita-Horn overlap index (MOI) is shown for each individual patient. (B) Percentage of TCR β -chain CDR3 clonotypes differentially expressed between pre- and on-therapy samples from the total number of clonotypes present in each patient ($n = 5$). TCR β -chain CDR3 clonotypes that are significantly overrepresented in the on- and pretherapy are indicated in red and blue, respectively. (C) Bar graph illustrating the difference in V-segment usage distribution (Jensen-Shannon divergence [JSD]) between pre- and on-therapy samples for individual patients ($n = 5$). (D) Bar graph illustrating the difference in CDR3 length distribution (JSD) between pre- and on-therapy samples for individual patients ($n = 5$). (E) TCR clonality (1-normalized Shannon-Wiener index) in pre- and on-therapy samples. Statistical significance between pre- and on-therapy samples was tested with a two-tailed Wilcoxon signed-rank test, $P = 0.19$.

treatment in contrast to 56% of patients treated without prior anti-CTLA-4 therapy (*SI Appendix, Fig. S6F*; $P = 0.12$). These findings may reflect a broadening upon anti-CTLA-4 therapy as shown in our previous study (21) and current work (see *Differential Effects of CTLA-4 and PD-1 Blockade on the Melanoma-Reactive CD8 T Cell Response*). Lastly, previous studies have shown an increase of proliferating (Ki-67⁺) CD8 T cell subsets within bulk CD8 T cells in the first weeks during anti-PD-1 therapy (14–17). To further validate our patient cohort, we assessed the effects of PD-1 blockade on Ki-67⁺ PD-1⁺ CD8 T cells in peripheral blood samples from five patients before and during treatment (week 1 and weeks 9 to 12). In line with previous studies (14–17), we observed a consistent increase of Ki-67⁺ PD-1⁺ CD8 T cells at week 1 ($P = 0.007$) in all five patients (*SI Appendix, Fig. S7*). Together, these results demonstrate that the response profile of the analyzed patient cohort and the effects of anti-PD-1 therapy on the

kinetics of a proliferating CD8 T cell subset were comparable to previous studies and that alterations of the circulating melanoma-reactive CD8 T cell response upon PD-1 blockade do not appear to be correlated with the clinical activity of the treatment or prior anti-CTLA-4 therapy.

Differential Effects of CTLA-4 and PD-1 Blockade on the Melanoma-Reactive CD8 T Cell Response. Our current results demonstrate that PD-1 blockade does not measurably influence the melanoma-reactive CD8 T cell response in peripheral blood. In contrast, in prior work, we demonstrated that anti-CTLA-4 therapy induces broadening of the melanoma-reactive CD8 T cell repertoire in peripheral blood (21). To understand whether this difference in the therapy effects on circulating CD8 T cells holds true in-patient cohorts that were treated with either PD-1 or CTLA-4 blockade and analyzed concurrently using the same technology and reagents, we analyzed samples from nine

Table 1. Demographic and clinical characteristics of the analyzed patient cohort treated with anti-PD-1 therapy

Total number of patients (n = 24)	
Median age, years (range)	53 (31 to 87)
Gender, n (%)	
Female	10 (41%)
Male	14 (59%)
Anti-PD-1 therapy, n (%)	
Pembrolizumab	22 (92%)
Nivolumab	2 (8%)
CNS metastasis, n (%)	
Yes	5 (21%)
No	19 (79%)
WHO performance status, n (%)	
NA	6 (25%)
0	12 (50%)
1	6 (25%)
LDH level before first dose of anti-PD-1 therapy, n (%)	
<ULN	18 (75%)
1 to 2 ULN	3 (12.5%)
>2 ULN	3 (12.5%)
BRAF mutation, n (%)	
Yes	8 (33%)
No	16 (67%)
Previous therapies, n (%)	
BRAF or BRAF/MEK inhibitors	5 (21%)
Anti-CTLA-4 therapy*	14 (58%)
Best overall response to anti-PD-1 therapy, n (%)	
NA	1 (4%)
CR	4 (17%)
PR	8 (33%)
SD	5 (21%)
PD	6 (25%)

CR, complete response; PR, partial response; SD, stable disease; PD, progressive disease; NA, not available; WHO, World Health Organization; BRAF, v-raf murine sarcoma viral oncogene homolog B1; MEK, mitogen-activated protein kinase kinase; LDH, lactate dehydrogenase; ULN, upper limit of normal; CNS, central nervous system.

*Time between last dose of anti-CTLA-4 and first dose of anti-PD-1 therapy, median: 6, and range: 1 to 24 mo.

melanoma patients treated with CTLA-4 blockade (clinical characteristics shown in *SI Appendix, Table S3*). We have previously shown that anti-CTLA-4 therapy does not influence the magnitude of preexisting responses during treatment and that newly detectable responses were detectable early during treatment and remained stable up to several months after the start of therapy (21). Peripheral blood samples were therefore collected pretherapy and posttherapy (~12 wk after start of treatment at the time of the first clinical evaluation). In total, 13 melanoma-reactive CD8 T cell responses were identified in eight out of nine patients with a median magnitude of 0.028%, ranging from 0.006 to 0.363% (Fig. 5A and B). In concordance with our prior analyses (21), the magnitude of preexisting, melanoma-reactive CD8 T cell responses was unaltered after anti-CTLA-4 therapy, with a median fold change of 0.9 (Fig. 5C and *SI Appendix, Fig. S8*). Importantly, however, and in line with prior analyses (21), a broadening of the melanoma-reactive CD8 T cell repertoire was observed in five out of nine melanoma patients (56%). Of note, two viral epitopes derived from the Epstein-Barr virus and influenza A were included in the analysis as a technical control for the generation of pMHC multimers, and virus-specific CD8 T cell responses were detected in eight of the nine patients (*SI Appendix, Fig. S3C*).

In summary, the parallel analysis using the same technology and reagents showed a broadening of the circulating, melanoma-reactive CD8 T cell repertoire upon CTLA-4 blockade, and such a broadening was observed significantly more frequently in patients treated with anti-CTLA-4 than anti-PD-1 therapy (Fig. 5D; $P = 0.02$).

Discussion

The clinical success of anti-PD-1 therapy, in particular for advanced melanoma patients, and the importance of CD8 T cells in tumor control has led to a major interest in understanding the mechanism of action on CD8 T cells. Several studies observed systemic alterations of the bulk CD8 T cell compartment upon PD-1 blockade (14–18); however, direct evidence demonstrating a systemic effect on the tumor-reactive CD8 T cell response is currently lacking. To address this question, we measured the impact of the treatment on the circulating, melanoma-reactive CD8 T cell response directly ex vivo and compared these findings to the effects of CTLA-4 blockade.

Boosting or broadening of the melanoma-reactive CD8 T cell response upon PD-1 blockade was not observed in the vast majority of patients despite the objective clinical response rate of 50%. In line with previous studies (14–17), the frequency of a small subset of proliferating PD-1⁺ Ki67⁺ CD8 T cells was increased in the first week after the start of anti-PD-1 therapy, which may reflect proliferation of CD8 T cells with other antigen specificities. However, given the low frequency (median: 0.15% and range: 0.013 to 2.85% of PD-1⁺ Ki67⁺ cells of total CD8 T cells), their importance for tumor control remains to be established in future studies. The lack of boosting or broadening of the circulating, melanoma-reactive CD8 T cell response was in line with the absence of prominent changes of the TCR repertoire of circulating CD8 T cells upon anti-PD-1 therapy; a finding which is in line with a previous study (19). Furthermore, analysis of gp100-specific CD8 T cells of two melanoma patients showed expansion of tumor-reactive CD8 T cells upon PD-1 blockade in the tumor, whereas an expansion of the T cell response was detected infrequently in peripheral blood (16). Contrary to previous studies suggesting a potential role of PD-1 blockade in the priming of novel CD8 T cell responses or reactivation of preexisting CD8 T cell responses (10–13), our data show that PD-1 blockade does not significantly increase the breadth of the melanoma-reactive CD8 T cell response. In line with these findings, a recent study demonstrated that anti-PD-1 therapy as monotherapy is insufficient for the priming of naive, tumor-reactive CD8 T cells in a mouse model (27). Furthermore, our previous (21) and current analysis using the same technology showed that in contrast to PD-1 blockade, CTLA-4 blockade increases the breadth of the melanoma-reactive CD8 T cell repertoire in peripheral blood.

The current study has the following limitations. While our analyses involve the measurement of 71 potential CD8 T cell responses, it is limited to shared melanoma antigens restricted to the HLA-A*02:01 allele. We focused on HLA-A*02:01 because most of previously identified, melanoma-associated antigens are restricted by this allele. Despite the focus on only one of the potentially six different HLA alleles of each patient, melanoma-reactive CD8 T cell responses were identified in the vast majority (79%) of patients. The focus on shared melanoma antigens rather than patient-specific neoantigens may, however, lead us to underestimate the effects of immune checkpoint blockade, as differences in TCR affinity may influence the effects of PD-1 blockade on shared tumor- versus neoantigen-specific CD8 T cells. However, data from a tumor mouse model have shown that anti-PD-1 therapy enhanced tumor control of both high- and low-affinity ligand-expressing tumors (28). Furthermore, the observation that a broadening of the CD8 T cell

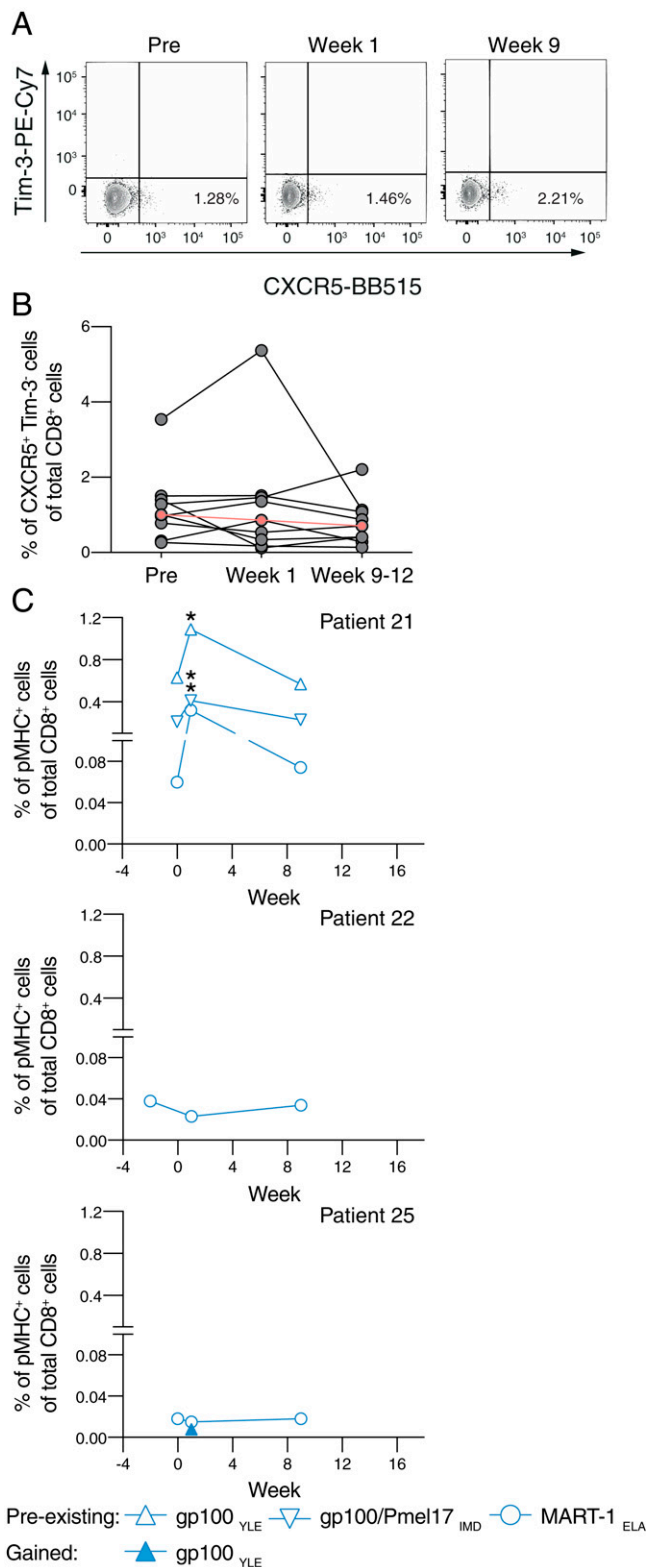


Fig. 4. Assessment of (melanoma reactive) CD8 T cells at week 1 after PD-1 blockade. (A) Representative flow cytometry plots showing the kinetics of bulk CXCR5⁺ Tim-3⁻ CD8 T cells. The frequency is shown on the top left for each time point. (B) Kinetics of CXCR5⁺ Tim-3⁻ bulk CD8 T cells for individual patients ($n = 8$, gray) following anti-PD-1 therapy. The median (red) for each individual time point is shown. Statistical significance was tested with a Friedman's test with Dunn's post hoc: pretherapy versus week 1: $P > 0.99$ and pretherapy versus week 9 to 12: $P = 0.19$. (C) Kinetics of melanoma-reactive CD8 T cell responses detected in melanoma patients

response against shared melanoma antigens is observed upon CTLA-4 blockade in the current study and our previous work (21) argues for the validity of our approach in detecting global therapy-induced alterations. While the current data argue against a profound effect of PD-1 blockade on the circulating, tumor-reactive CD8 T cell compartment, we observed newly detectable CD8 T cell responses upon PD-1 blockade in 3 of the 24 analyzed patients. In addition, we have previously reported a newly detectable, neoantigen-specific CD8 T cell response upon anti-PD-1 therapy in an NSCLC patient (29). Whether this represents a modest effect of PD-1 blockade on the breadth of the circulating, tumor-reactive CD8 T cell response will require analysis of a substantially larger patient cohort. However, the absence of prominent changes of the TCR repertoire observed in our and previous work (19) argues against the possibility that PD-1 blockade induces significant alterations of the circulating, tumor-reactive CD8 T cell response regardless of antigen specificity. Overall, based on the current evidence, it can be concluded that the broadening of the circulating, tumor-reactive CD8 T cell repertoire upon PD-1 blockade is rare compared to CTLA-4 blockade. Based on this observation and the fact that the clinical activity of PD-1 blockade is higher than that of CTLA-4 blockade, it may be argued that a substantial part of the immunomodulatory effect of PD-1 blockade occurs at the tumor site, potentially including draining lymph nodes and tertiary lymphoid structures within the tumor.

In summary, this study demonstrates that contrary to CTLA-4 blockade, PD-1 blockade does not lead to significant alterations of circulating CD8 T cells with a defined tumor specificity despite a substantially higher clinical activity of PD-1 compared to CTLA-4 blockade (30). Our findings provide in-depth information about the mode of action of checkpoint-targeting therapies on the circulating, tumor-specific CD8 T cell response that can be utilized as rationale for new combination treatment strategies. In future work, it will be of interest to investigate the effect of anti-PD-1 therapy on defined tumor-reactive CD8 T cell populations at the tumor site. We note, however, that the high variability in the presence and magnitude of tumor-reactive CD8 T cells even between tumor fragments of the same tumor piece (22) is likely to limit the ability to detect therapy-induced alterations in pre- and posttreatment biopsies. Conceivably, analysis of the cell cycle state of intratumoral, tumor-reactive CD8 T cells identified using the pMHC multi-mer technology (31) may form a more sensitive approach.

Materials and Methods

Patient Material. Peripheral blood mononuclear cell (PBMC) samples were obtained from stage IV melanoma patients undergoing immune checkpoint-targeting therapy either at The Netherlands Cancer Institute, the University of California, Los Angeles, or the University Hospital Essen. The patient cohort treated with anti-PD-1 therapy received either pembrolizumab 2 mg/kg or a fixed dose of 150 to 200 mg intravenously every 3 wk or nivolumab 3 mg/kg or in a fixed dose of 240 mg intravenously every 2 wk in an expanded access program or according to the label after approval. The patient cohort treated with anti-CTLA-4 therapy received ipilimumab intravenously in a dose of 3 mg/kg every 3 wk for a maximum of four cycles. Clinical response was evaluated according to response evaluation criteria in solid tumors version 1.1 (32). The study was conducted in accordance with the Declaration of Helsinki after approval by the institutional review boards of all centers. PBMC samples were collected in accordance with local guidelines and following signed informed consent. PBMCs were isolated using standard Ficoll-Plaque density centrifugation according to local operating procedures. After isolation, PBMCs were cryopreserved in liquid nitrogen, in fetal calf serum (Sigma F7524) with dimethyl sulfoxide (Sigma,

$n = 3$) following anti-PD-1 therapy. A \geq twofold increase (on-therapy versus pretherapy) in magnitude is indicated (*). A representative example of the full gating strategy is shown in *SI Appendix, Fig. S5*.

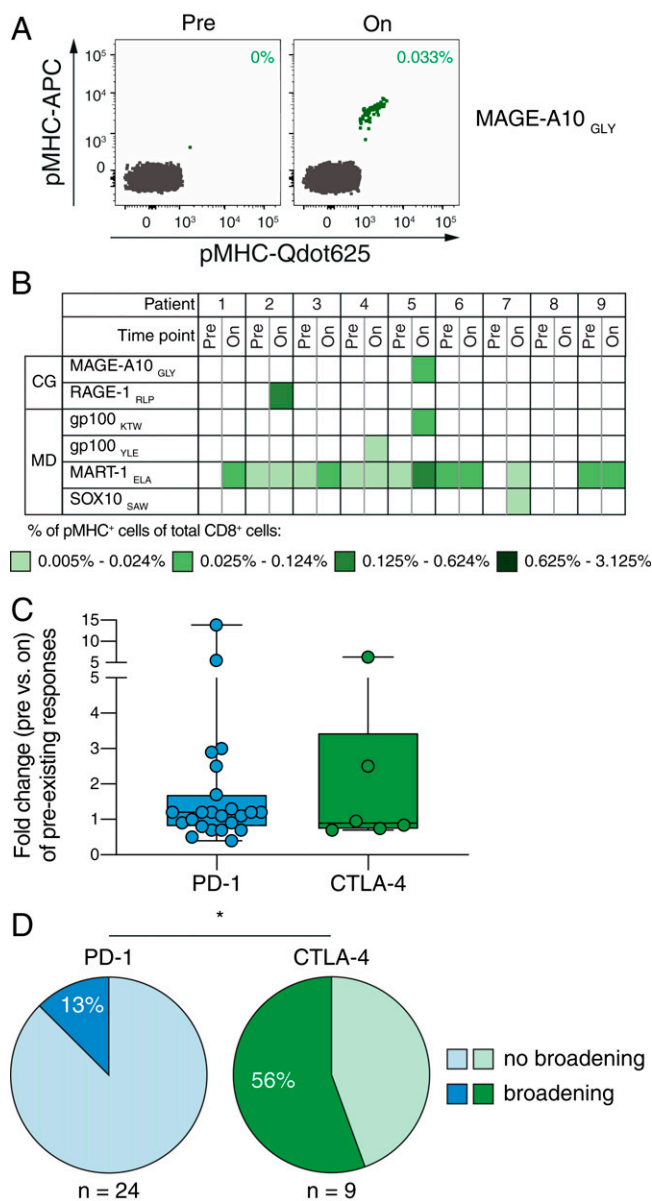


Fig. 5. Assessment of differential alterations of the melanoma-reactive CD8 T cell response upon PD-1 and CTLA-4 blockade. (A) Representative flow cytometry plots of a gained, melanoma-reactive CD8 T cell response (green) detected in peripheral blood upon CTLA-4 therapy. Magnitude of the melanoma-reactive CD8 T cell response (green, upper corner) is indicated on the top right as the percentage of total CD8 T cells (gray). Full gating strategy is provided in *SI Appendix, Fig. S1*. (B) Heatmap overview of melanoma-reactive CD8 T cell responses ($n = 13$) detected in melanoma patients ($n = 9$) before and after (median: week 9 and range: week 6 to 22) anti-CTLA-4 therapy. C/G: cancer/germline, MD: melanocyte differentiation. (C) Fold change in magnitude of preexisting, melanoma-reactive CD8 T cell responses detected in patients treated with anti-PD-1 ($n = 23$) or anti-CTLA-4 ($n = 6$) therapy. Boxplots represent the median and interquartile ranges, and the whiskers represent the full range. Statistical significance between the two groups was tested with a two-tailed Mann-Whitney U test, $P = 0.76$. (D) Proportion of patients with zero (no broadening) or \geq one newly detectable (broadening) melanoma-reactive CD8 T cell responses after anti-PD-1 therapy (blue) or after anti-CTLA-4 therapy (green). Statistical significance between the two groups was tested with a two-sided Fisher's exact test, $P = 0.02$.

D4540, 10% volume/volume). For the analysis of melanoma-reactive CD8 T cell responses, patients were selected based on four-digit genotyping for HLA-A*02:01. Therefore, DNA was isolated using the DNeasy Blood & Tissue Kit

(Qiagen, 69506) according to manufacturer's protocol (Qiagen), and HLA typing was done using next-generation sequencing according to the manufacturer's protocol (GenDx).

Epitopes. Melanoma-reactive CD8 T cell responses were identified using an HLA-A*02:01-restricted epitope panel, including 71 epitopes (*SI Appendix, Table S1*) derived from shared melanoma antigens. As positive control for the generation of pMHC multimers, two viral epitopes derived from the Epstein-Barr virus and influenza A were included in the epitope panel (*SI Appendix, Fig. S3*). Peptides derived from shared melanoma-associated, viral antigens as well as ultraviolet (UV)-cleavable peptides were synthesized at the Division of Chemical Immunology, Leiden University Medical Center, as previously published (33).

Generation of pMHC Multimers. MHC HLA-A*02:01 allele monomers were generated with a UV-cleavable epitope as previously published (33). Specific pMHC complexes used for the identification of antigen-specific CD8 T cell responses were generated by UV-induced ligand as previously described (31). In brief, MHC monomers loaded with UV-cleavable peptide were exposed to 254/366 nm UV light for 1 h at 4 °C in the presence of a specific rescue peptide (200 μ M). Subsequently, fluorochrome streptavidin reagents (*SI Appendix, Table S4*) were conjugated to pMHC monomers (100 μ g/mL). For data acquisition on the BD LSRII, conjugation was performed with two of the 10 fluorochrome streptavidin reagents resulting in dual fluorescent color codes for up to 37 epitopes. For data acquisition on the BD FACSymphony, conjugation was performed with 2 of the 14 fluorochrome streptavidin reagents, resulting in dual fluorescent color codes for up to 74 epitopes. Subsequently, fluorescently labeled pMHC multimers were incubated for 30 min on ice. D-biotin (Sigma, B4501, 26.3 mM) and NaN_3 (0.02% weight/volume) in phosphate-buffered saline was added to block residual binding sites.

Flow Cytometry Assays. PBMCs were thawed and recovered in Roswell Park Memorial Institute 1640 (Life Technologies, 21875-034) supplemented with human serum (Sigma, H3667, 10% volume/volume), penicillin-streptomycin (Life Technologies, 15140-122, 1% volume/volume), and benzonase nuclease (Merck-Millipore, 70746-4, 2,500 U/mL), resuspended, and incubated at 37 °C for 30 min before staining. For the pMHC multimer assay, antigen-specific CD8 T cells were stained for 15 min at 37 °C with pMHC multimers (*SI Appendix, Table S5*). Subsequently, cells were stained for 20 min on ice with antibodies (*SI Appendix, Table S5*) and LIVE/DEAD Fixable IR Dead Cell Stain Kit (Invitrogen, L10119, 1/200). For the acquisition on the BD FACSymphony, individual staining was performed in the presence of Brilliant Staining Buffer Plus (BD, 563794) according to manufacturer's protocol (BD). All samples were washed twice before acquisition and analyzed on the BD LSRII. A subset of samples was analyzed on both the BD LSRII and the BD FACSymphony to confirm consistency between the two instruments. Antigen-specific CD8 T cell responses were confirmed using a different dual color-code fluorochrome combination in each of the two independent experiments, the initial screen, and the confirmation. An analysis of surface (Tim-3, CXCR5, and PD-1) and intracellular (Ki-67) markers on CD8 T cells was only assessed on the BD FACSymphony because of better detection sensitivity compared to BD LSRII. To assess expression of Ki-67 and PD-1 on CD8 T cells, cells were first washed and stained for 20 min on ice with surface marker antibodies (*SI Appendix, Table S5*). After washing, cells were stained for 10 min on ice with LIVE/DEAD Fixable IR Dead Cell Stain Kit (Invitrogen, L10119, 1/400). Subsequently, cells were washed, fixed, and permeabilized using the Foxp3 Transcription Factor Staining Buffer Set (eBioscience, 00-5523-00) according to manufacturer's protocol, and Ki-67 staining was performed for 20 min on ice (*SI Appendix, Table S5*). All samples were washed twice before acquisition.

Identification of Antigen-Specific CD8 T Cell Responses. An analysis of antigen-specific CD8 T cell responses was carried out without prior knowledge about clinical patient characteristics to avoid experimental bias. The following gating strategy was applied to identify CD8 T cells: 1) selection of live single-cell CD8 T cells, 2) selection of pMHC⁺ live single-cell CD8 T cells, and 3) selection of antigen-specific CD8 T cells that were positive for two, and none of the other fluorescent pMHC multimers were identified using Boolean gating (21, 34, 35). The full gating strategy used on the BD LSRII and the BD FACSymphony is shown in *SI Appendix, Figs. S1 and S5*, respectively. Cutoff values for the definition of positive responses were $\geq 0.005\%$ of total CD8 T cells and ≥ 10 events in both experiments, the initial screen, and the confirmation. A minimum of 50,000 CD8 T cells were acquired per sample. To reduce person bias of manual gating, only positive responses that were confirmed by two independent people in both experiments were defined as real (*SI Appendix, Fig. S1 B and C*). The average response magnitude that was determined by two independent people from the initial screen was used for statistical

analysis. Data were analyzed using either the BD FACSDiva (version 8.0.1) or the FlowJo (version 10.5.3) software. To monitor the reproducibility of the assay system, reference samples with up to 10 CD8 T cell responses present at varying frequencies were included in each analysis.

Flow Cytometer Settings. On the BD LSRII, the following 13-color instrument settings were used: Blue laser (488 nm at 100 mW): fluorescein isothiocyanate, 505LP, and 525/50BP. Red laser (637 nm at 40 mW): allophycocyanin (APC) and 670/14BP; AF700, 685LP, and 710/50BP; and IRDye, 750LP, and 780/60BP. Violet laser (405 nm at 100 mW): BV421 and 450/50BP; QD625, 610LP, and 625/20BP; and QD655, 635LP, and 655/8BP. UV laser (355 nm at 20 mW): QD585, 570LP, and 5812/15BP; QD605, 595LP, and 605/12BP; QD705, 685LP, and 710/50BP; and QD800, 750LP, and 780/60BP. Yellow-green laser (561 nm at 50 mW): phycoerythrin (PE), 585/15BP, PE-Cy7, 795LP, and 780/60BP. On the BD FACSymphony, the following 18-color instrument settings were used: Blue laser (488 nm at 200 mW): BB515, 505LP, and 530/30BP; BB630, 600LP, and 610/20BP; PerCP-Cy5.5, 685LP, and 710/50; and BB790, 750LP, and 780/60BP. Red laser (637 nm at 140 mW): APC, 670/30BP, APC-R700, 690LP, 630/45BP, and IRDye and APC-H7, 750LP, and 780/60BP. Violet laser (405 nm at 100 mW): BV421, 420LP, and 431/28BP; BV480, 455LP, and 470/20BP; BV605, 565LP, and 605/40BP; BV650, 635LP, and 661/11BP; and BV750, 735LP, and 750/30BP. UV laser (355 nm at 75 mW): BUV395, 379/28BP, BUV563, 550LP, 580/20BP; BUV615, 600LP, and 615/20BP and BUV805, 770LP, and 819/44BP. Yellow-green laser (561 nm at 150 mW): PE and 586/15BP; BYG670, 635LP, and 670/30BP; and PE-Cy7, 750LP, and 780/60BP. Appropriate compensation controls were included in each analysis.

TCR Sequencing. TCR beta chain CDR3 region sequencing was performed on CD8 T cells isolated from pre- and on-therapy PBMC samples to assess changes in the TCR repertoire upon PD-1 blockade. PBMCs were thawed and recovered as described above (see *Flow Cytometry Assays*). Subsequently, CD8 T cells were isolated using the CD8 T cell isolation kit (MACS Miltenyi Biotec, 130-096-495) and LS columns (MACS Miltenyi Biotec, 130-042-401) according to the manufacturers protocol, and DNA was isolated using the QiAMP DNA Micro Kit (Qiagen, 56304) according to the manufacturers protocol. TCR sequencing was performed using the immunoSEQ Assay from Adaptive Biotechnologies with survey resolution. Python 3.7.6 (36), Pandas 1.0.1 (37), NumPy 1.18.1 (37), and SciPy 1.4.1 (38) were used for data analysis. VDJtools 1.2.1 (39) was used for the TCR sequencing data analysis. The clonotype data

were exported from the Adaptive immunoSEQ Analyzer using Export samples v2 option and converted to VDJtools format using VDJtools Convert routine. Clonality was estimated as 1-normalized Shannon–Wiener index. Normalized Shannon–Wiener index values were computed using VDJtools CalcDiversityStats routine with default parameters performing resampling. CDR3 length distributions and V-segment usage distributions were obtained with VDJtools CalcSpectratype and VDJtools CalcSegmentUsage routine, respectively, using default parameters. The matching of the TCR repertoire of the patients with a public epitope database was performed with VDJmatch (40) using full VDJmatch algorithm scoring and weighting database hits by their informativeness. Only hits with scores equal to 2 or 3 were used in the subsequent analysis. Differential expression of clonotypes between pre- and on-therapy samples was assessed using the Adaptive immunoSEQ Analyzer Differential Abundance tool, on nucleotide level, with minimum clone abundance of 5 and beta binomial *P* value estimation method.

Statistical Analysis. Wilcoxon matched-pairs signed-rank test was used to assess changes in the number and magnitude of antigen-specific CD8 T cell responses detected pre- and on/after therapy. Differences between patient groups were assessed using the nonparametric Mann–Whitney *U* test. Statistical significance for associations between categorical variables was determined by Fisher's exact test. Statistical analysis was performed using Excel (version 16.36) and Prism 8 (version 8.1.2).

Data Availability. Flow cytometry data generated in the study are deposited on FlowRepository (<http://flowrepository.org/id/FR-FCM-Z48G>) (41). TCR sequencing data generated in this study are deposited in the immuneACCESS Data repository (<https://doi.org/10.21417/AG2021PNAS>) (42). All other data are included in the article and *SI Appendix*.

ACKNOWLEDGMENTS. We thank M. van Baalen, A. Pfauth, and F. van Diepen for their flow cytometric support. We thank R. Balderas from BD Biosciences, C. Talavera from the University of Leiden, and M. Toebes and M. van den Braber from The Netherlands Cancer Institute for providing us with essential reagents for our experiments. We thank The Netherlands Cancer Institute–Antoni van Leeuwenhoek (NKI-AVL) Core Facility Molecular Pathology & Biobanking for their support and for supplying us with NKI-AVL Biobank material. The research was funded by the Koningin Wilhelmina Fonds Dutch Cancer Society and Merck.

1. C. Robert *et al.*, Nivolumab in previously untreated melanoma without BRAF mutation. *N. Engl. J. Med.* **372**, 320–330 (2015).
2. H. Borghaei *et al.*, Nivolumab versus docetaxel in advanced nonsquamous non-small-cell lung cancer. *N. Engl. J. Med.* **373**, 1627–1639 (2015).
3. R. J. Motzer *et al.*; CheckMate 025 Investigators, Nivolumab versus everolimus in advanced renal-cell carcinoma. *N. Engl. J. Med.* **373**, 1803–1813 (2015).
4. T. Powles *et al.*, Atezolizumab versus chemotherapy in patients with platinum-treated locally advanced or metastatic urothelial carcinoma (IMvigor211): A multicentre, open-label, phase 3 randomised controlled trial. *Lancet* **391**, 748–757 (2018).
5. P. C. Tumeh *et al.*, PD-1 blockade induces responses by inhibiting adaptive immune resistance. *Nature* **515**, 568–571 (2014).
6. J. Larkin *et al.*, Combined nivolumab and ipilimumab or monotherapy in untreated melanoma. *N. Engl. J. Med.* **373**, 23–34 (2015).
7. S. L. Topalian *et al.*, Safety, activity, and immune correlates of anti-PD-1 antibody in cancer. *N. Engl. J. Med.* **366**, 2443–2454 (2012).
8. T. Noguchi *et al.*, Temporally distinct PD-L1 expression by tumor and host cells contributes to immune escape. *Cancer Immunol. Res.* **5**, 106–117 (2017).
9. J. W. Kleinovink *et al.*, PD-L1 expression on malignant cells is no prerequisite for checkpoint therapy. *Oncol Immunology* **6**, e1294299 (2017).
10. S. J. Im *et al.*, Defining CD8+ T cells that provide the proliferative burst after PD-1 therapy. *Nature* **537**, 417–421 (2016).
11. R. He *et al.*, Follicular CXCR5-expressing CD8(+) T cells curtail chronic viral infection. *Nature* **537**, 412–428 (2016).
12. A. O. Kamphorst *et al.*, Rescue of exhausted CD8 T cells by PD-1-targeted therapies is CD28-dependent. *Science* **355**, 1423–1427 (2017).
13. E. Hui *et al.*, T cell costimulatory receptor CD28 is a primary target for PD-1-mediated inhibition. *Science* **355**, 1428–1433 (2017).
14. A. O. Kamphorst *et al.*, Proliferation of PD-1+ CD8 T cells in peripheral blood after PD-1-targeted therapy in lung cancer patients. *Proc. Natl. Acad. Sci. U.S.A.* **114**, 4993–4998 (2017).
15. A. C. Huang *et al.*, T-cell invigoration to tumour burden ratio associated with anti-PD-1 response. *Nature* **545**, 60–65 (2017).
16. A. C. Huang *et al.*, A single dose of neoadjuvant PD-1 blockade predicts clinical outcomes in resectable melanoma. *Nat. Med.* **25**, 454–461 (2019).
17. S. C. Wei *et al.*, Combination anti-CTLA-4 plus anti-PD-1 checkpoint blockade utilizes cellular mechanisms partially distinct from monotherapies. *Proc. Natl. Acad. Sci. U.S.A.* **116**, 22699–22709 (2019).
18. K. E. Yost *et al.*, Clonal replacement of tumor-specific T cells following PD-1 blockade. *Nat. Med.* **25**, 1251–1259 (2019).
19. L. Robert *et al.*, Distinct immunological mechanisms of CTLA-4 and PD-1 blockade revealed by analyzing TCR usage in blood lymphocytes. *Oncol Immunology* **3**, e29244 (2014).
20. M. M. Gubin *et al.*, Checkpoint blockade cancer immunotherapy targets tumour-specific mutant antigens. *Nature* **515**, 577–581 (2014).
21. P. Kvistborg *et al.*, Anti-CTLA-4 therapy broadens the melanoma-reactive CD8+ T cell response. *Sci. Transl. Med.* **6**, 254ra128 (2014).
22. P. Kvistborg *et al.*, TIL therapy broadens the tumor-reactive CD8(+) T cell compartment in melanoma patients. *Oncol Immunology* **1**, 409–418 (2012).
23. B. C. Miller *et al.*, Subsets of exhausted CD8+ T cells differentially mediate tumor control and respond to checkpoint blockade. *Nat. Immunol.* **20**, 326–336 (2019).
24. I. Siddiqui *et al.*, Intratumoral Tcf1+PD-1+CD8+ T cells with stem-like properties promote tumor control in response to vaccination and checkpoint blockade immunotherapy. *Immunity* **50**, 195–211.e10 (2019).
25. A. Ribas, J. D. Wolchok, Cancer immunotherapy using checkpoint blockade. *Science* **359**, 1350–1355 (2018).
26. J. S. Weber *et al.*, Sequential administration of nivolumab and ipilimumab with a planned switch in patients with advanced melanoma (CheckMate 064): An open-label, randomised, phase 2 trial. *Lancet Oncol.* **17**, 943–955 (2016).
27. V. Verma *et al.*, PD-1 blockade in subprimed CD8 cells induces dysfunctional PD-1+CD38hi cells and anti-PD-1 resistance. *Nat. Immunol.* **20**, 1231–1243 (2019).
28. A. Martinez-Usatorre, A. Donda, D. Zehn, P. Romero, PD-1 blockade unleashes effector potential of both high- and low-affinity tumor-infiltrating T cells. *J. Immunol.* **201**, 792–803 (2018).
29. N. A. Rizvi *et al.*, Cancer immunology. Mutational landscape determines sensitivity to PD-1 blockade in non-small cell lung cancer. *Science* **348**, 124–128 (2015).
30. F. S. H. Hodi *et al.*, Nivolumab plus ipilimumab or nivolumab alone versus ipilimumab alone in advanced melanoma (CheckMate 067): 4-year outcomes of a multicentre, randomised, phase 3 trial. *Lancet Oncol.* **19**, 1480–1492 (2018).
31. B. Rodenko *et al.*, Generation of peptide-MHC class I complexes through UV-mediated ligand exchange. *Nat. Protoc.* **1**, 1120–1132 (2006).
32. E. A. Eisenhauer *et al.*, New response evaluation criteria in solid tumours: Revised RECIST guideline (version 1.1). *Eur. J. Cancer* **45**, 228–247 (2009).
33. M. Toebes *et al.*, Design and use of conditional MHC class I ligands. *Nat. Med.* **12**, 246–251 (2006).

34. R. S. Andersen *et al.*, Parallel detection of antigen-specific T cell responses by combinatorial encoding of MHC multimers. *Nat. Protoc.* **7**, 891–902 (2012).
35. S. R. Hadrup *et al.*, Parallel detection of antigen-specific T-cell responses by multidimensional encoding of MHC multimers. *Nat. Methods* **6**, 520–526 (2009).
36. G. Van Rossum, F. L. Drake, *Python 3 Reference Manual* (CreateSpace, Scotts Valley, CA, 2009).
37. C. R. Harris *et al.*, Array programming with NumPy. *Nature* **585**, 357–362 (2020).
38. P. Virtanen *et al.*; SciPy 1.0 Contributors, SciPy 1.0: Fundamental algorithms for scientific computing in Python. *Nat. Methods* **17**, 261–272 (2020).
39. M. Shugay *et al.*, VDJtools: Unifying post-analysis of T cell receptor repertoires. *PLoS Comput. Biol.* **11**, e1004503 (2015).
40. M. Shugay *et al.*, VDJdb: A curated database of T-cell receptor sequences with known antigen specificity. *Nucleic Acids Res.* **46**, D419–D427 (2018).
41. A. Gangaev *et al.*, Differential effects of PD-1 and CTLA-4 blockade on the melanoma-reactive CD8 T cell response. FlowRepository. <http://flowrepository.org/id/FR-FCM-Z48G>. Deposited 1 July 2021.
42. A. Gangaev *et al.*, Differential effects of PD-1 and CTLA-4 blockade on the melanoma-reactive CD8 T cell response. immuneACCESS. <https://doi.org/10.21417/AG2021PNAS>. Deposited 1 July 2021.